

# Network topologies for maximal organismal health span and lifespan

Cite as: Chaos 33, 023124 (2023); doi: 10.1063/5.0105843

Submitted: 25 June 2022 · Accepted: 23 January 2023 ·

Published Online: 15 February 2023



View Online



Export Citation



CrossMark

Garrett Stubbings<sup>1</sup> and Andrew Rutenberg<sup>2</sup>

## AFFILIATIONS

Department of Physics and Atmospheric Science, Dalhousie University, Halifax, Nova Scotia B3H 4R2, Canada

<sup>a)</sup> Author to whom correspondence should be addressed: [Andrew.Rutenberg@dal.ca](mailto:Andrew.Rutenberg@dal.ca)

## ABSTRACT

The population dynamics of human health and mortality can be jointly captured by complex network models using scale-free network topology. To validate and understand the choice of scale-free networks, we investigate which network topologies maximize either lifespan or health span. Using the Generic Network Model (GNM) of organismal aging, we find that both health span and lifespan are maximized with a “star” motif. Furthermore, these optimized topologies exhibit maximal lifespans that are not far above the maximal observed human lifespan. To approximate the complexity requirements of the underlying physiological function, we then constrain network entropies. Using non-parametric stochastic optimization of network structure, we find that disassortative scale-free networks exhibit the best of both lifespan and health span. Parametric optimization of scale-free networks behaves similarly. We further find that higher maximum connectivity and lower minimum connectivity networks enhance both maximal lifespans and health spans by allowing for more disassortative networks. Our results validate the scale-free network assumption of the GNM and indicate the importance of disassortativity in preserving health and longevity in the face of damage propagation during aging. Our results highlight the advantages provided by disassortative scale-free networks in biological organisms and subsystems.

Published under an exclusive license by AIP Publishing. <https://doi.org/10.1063/5.0105843>

**Network models of aging have assumed that binary health attributes interact through a scale-free network topology. Empirical reconstruction of interaction networks large enough to test this scale-free assumption is not yet possible. Here, we instead search for topologies that maximize lifespan or health span—health throughout the lifespan. Our optimal networks are a simple star motif, and by imposing a fixed network entropy target, we obtain similar health and longevity but with a scale-free network topology. We use the target entropy to approximate the functional requirements of the organism. Our results validate the use of scale-free topologies in network models of aging health and indicate a generic advantage of disassortative scale-free networks for biological systems in the face of propagating network damage during aging.**

## I. INTRODUCTION

Organismal aging is a complex dynamical process that ends in death. Summary measures of aging health differ significantly from each other,<sup>1</sup> which suggests that aging is multi-dimensional.

Indeed, only high-dimensional machine learning models can accurately predict individual aging health trajectories.<sup>2</sup> Models of aging that include many health attributes are, therefore, useful to better understand the aging process. Network models are well suited for dynamical models of aging health since they can explicitly capture interactions between health attributes.<sup>2–8</sup>

Human mortality rates grow exponentially with age, which is the Gompertz law of mortality.<sup>9</sup> Damage also accumulates increasingly rapidly, but stochastically, with age.<sup>10,11</sup> To jointly capture the dynamical increase in both mortality and damage within one model, the Generic Network Model (GNM) of aging assumes a scale-free network model of interacting health attributes.<sup>5–7</sup>

Scale-free networks are often used in biological models.<sup>12–14</sup> While it has been claimed that they may actually be rare,<sup>15</sup> their prevalence may be underestimated by finite size effects imposed by the small number of nodes available in most empirical studies.<sup>16</sup> Within aging research, while progress has been made in determining the network structure for both binarized<sup>8</sup> and non-binarized<sup>2</sup> aging health variables, empirical approaches have been limited to small networks with only dozens of nodes. As a result, observed organismal aging data have not been sufficient to reliably

infer network topology. Nevertheless, long-tailed degree distributions together with high disassortivity—as provided by scale-free networks,<sup>14,17</sup> which have power-law degree distributions  $P(k) \sim k^{-\alpha}$ —were required to replicate the observed mutual information between the damage of aging health attributes and mortality.<sup>7</sup>

While scale-free networks can describe aging phenomenology, it is not clear how or why they arise. A general critique of scale-free networks is that functional or generative mechanisms for how they arise are often missing.<sup>18</sup> This critique is important to address since such a functional mechanism could also apply to health at different scales of physiological function—i.e., subsystems, organs, and tissues. If such a mechanism exists, we might expect ubiquitous scale-free networks describing aging health.

What would a principled approach to network topology look like? While there are many detailed evolutionary theories of organismal aging,<sup>19–21</sup> they should all be consistent with high reproductive success over a natural life-course. Within the context of the GNM, where health attributes are not mapped to specific physiological functions, this is best represented by maximizing the time span of good health. We could also imagine that reproductive success is specifically preserved during natural lifespans, in which case we could simply maximize lifespan.

A healthy lifespan (health span) is of considerable interest in aging research.<sup>22</sup> While there are a variety of tools for assessing health span, the QALY (quality- or health-adjusted life-years) approach of weighting years of life by a health index between 0 and 1 is often used.<sup>23</sup> Here, we assume that organisms that are in better health for larger periods of time will be more successful, so we will take QALY as a proxy for evolutionary fitness. So, we are interested in how health span—as measured by QALY—is affected by network topology, and how it can be maximized.

There is also controversy about the limits of the human lifespan (see, e.g., Refs. 24–26). An interesting question in this context is how the maximal average lifespan obtained by optimizing the network topology compares to what we observe today.

Network connections (edges) in the GNM capture how the different health attributes of the organism are interdependent. The GNM models the propagation of damage or dysfunction, so the static network connections model how such dysfunction spreads. Nevertheless, it is reasonable to assume that interdependencies of dysfunction reflect interdependencies of function—and so are constrained by physiological function. Such constraints on the network structure could push it away from simply optimizing health span or lifespan performance. Maximizing entropy is a common approach in the face of unknown constraints.<sup>27,28</sup> Accordingly, we will constrain network entropy to approximate the unknown physiological constraints on network topology.

Often entropy has been used to characterize damage. The entropy of disorder has been used to describe genomic damage during aging,<sup>29</sup> while excess thermodynamic entropy production is a result of organismal dysfunction.<sup>30</sup> In contrast, here we use entropy to characterize the network of interactions that are present at maturity within the GNM. Damage propagates within the static network of interactions; the entropy reflects network complexity rather than damage.

We have four questions that we explore in this work. First, do different network topologies arise from optimizing longevity vs

health span? Second, are optimized network topologies similar to the scale-free networks used in GNM models of population aging?<sup>5–7</sup> Third, how does network entropy affect longevity or health span? Finally, what other aspects of network topology affect lifespan and health span? We consider all of these questions within the context of the dynamical GNM of aging, where we leave the parameters of the health dynamics unchanged during network optimization.

## II. METHODS

### A. Damage and mortality dynamics

In this work, we use the stochastic GNM dynamics<sup>7</sup> with a modified mortality condition (see below). Each of the  $N = 10^4$  nodes represents a binary health attribute of an individual that can be in either a healthy ( $d_i = 0$ ) or unhealthy ( $d_i = 1$ ) state. Nodes are dynamic while edges or links are static. Each individual starts with every node undamaged at age  $t = 0$ . Every node starts with the same basal damage rate  $\Gamma_0$ , so the initial damage in the network is independent of the structure. A node being damaged increases the damage rate of its neighboring nodes. That is, the damage rate of the  $i$ th node increases exponentially with the damage of its neighbors as follows:

$$\Gamma_i^+ = \Gamma_0 e^{\gamma^+ f_i}, \quad (1)$$

where  $f_i$  is the local frailty of the  $i$ th node—the FI measured over the neighbors (indexed  $j$ ),

$$f_i = \sum_{\text{neigh } j} d_j / k_i. \quad (2)$$

This results in damage spreading rapidly from nodes, which have damaged at early times due to the basal damage rate. Importantly, the nodes most susceptible to neighbor damage are low degree nodes since the damage rate increases exponentially with increments of  $1/k$ . So, the initial damage in the network spreads most quickly to the low degree nodes and then the neighbors of these low degree nodes. High degree nodes are not so heavily affected by neighbor damage and tend to damage later, which leads to the neighbors of these high degree nodes damaging later as well.

In this work, we use a proportional hazard model of mortality.<sup>31</sup> An individual's mortality rate increases exponentially with the average damage of their entire network  $f_{tot}$ ,

$$\Gamma_M = \Gamma_d e^{\gamma_m f_{tot}}, \quad (3)$$

where  $f_{tot} = \sum_{i=1}^N d_i / N$ . We find that using  $\Gamma_d = 0.01$ ,  $\gamma_m = 8$ ,  $\gamma_+ = 7.5$ , and  $\Gamma_0 = 0.00183 \text{ yr}^{-1}$ —together with a scale-free exponent  $\alpha = 2.35$  and average connectivity  $\langle k \rangle = 4$ —we retrieve the same human health and mortality statistics as previously reported for the GNM, which were shown to match observations.<sup>6,7</sup>

While proportional hazards mortality introduces two more model parameters ( $\Gamma_d$  and  $\gamma_m$ ) than the “two-node” mortality condition used previously,<sup>7</sup> we do not modify any of the dynamical parameters ( $\Gamma_d$ ,  $\gamma_m$ ,  $\gamma_+$ , or  $\Gamma_0$ ) during our optimization of the network topology. We also keep the average degree fixed, with  $\langle k \rangle = 4$ .

## B. Network generation

The space of distinct network topologies with  $N = 10^4$  nodes is huge and is impractical to effectively search and optimize without simplification. Accordingly, we consider degree distributions  $P(k)$  with minimum and maximum degree  $k_{\min} \geq 1$  and  $k_{\max} < N$ , respectively. Unless otherwise mentioned, we use  $k_{\min} = 2$  since it matches the minimum degree in the scale-free networks used in the original GNM work.

For a tractable non-parametric approach, we consider degree distributions  $P(k)$  with a specific selection of possible node degrees. At low degrees, we allow all  $k$  from  $k_{\min}$  to  $k = 6$ . Restricting the upper limit of this range to 4 or increasing it to 10 does not change our qualitative results. At higher degrees, we use log-uniform spacing from  $k = 6$  to  $k_{\max}$ . Using log- or linearly- randomly sampled degrees instead also does not change our qualitative results. In all, we use 15 possible node degrees. Using 10 or 20 instead does not change our qualitative results, though optimizing 20 or more distinct degrees becomes computationally onerous.

We sample the degree distributions using the random hubs method,<sup>32</sup> which is well suited to sampling long-tailed distributions while maintaining a precise  $\langle k \rangle$ . Our parametric optimization uses scale-free networks generated for a given exponent  $\alpha$  using a preferential attachment method to determine the degree counts of the network,  $D(k)$ .

Using the sampled degree counts  $D(k)$ , we build the joint connection matrix  $J(k', k)$  using tunable assortativity parameters  $p_d$ ,  $p_a$ , and  $p_r$  (with  $p_d + p_a + p_r = 1$ ). Beginning with the highest degree, we connect it to the furthest degree with probability  $p_d$  (disassortatively), to the most similar degree with probability  $p_a$  (assortatively), or to a random degree—weighted by remaining available connections—with probability  $p_r$ . Once all edges for nodes of degree  $k$  are satisfied, we repeat the process for the next largest  $k$  until all edges are assigned within  $J(k', k)$ .

Alongside the assortativity tuning, there are several constraints on how edges may be assigned in the network. We insist that networks must be fully connected—since all parts of the organism are in some capacity connected. Furthermore, the network must be simply connected, excluding self-connections that would effectively modify the damage rate of a node and so violate the generic assumption of the model. Similarly, multiple connections between nodes is also disallowed since they would violate the unweighted graph assumption; nodes with multiple connections would contribute to the damage rate according to the number of connections.

Once edges have been assigned consistent with constraints, the network is generated from  $J(k', k)$  using the method of Gjoka *et al.*<sup>33</sup>

We explore the network space with an evolutionary algorithm, making random changes to both the degree distribution  $P(k)$ —either directly in the non-parametric case or through the scale-free exponent  $\alpha$ —and the assortativity parameters ( $p_d$ ,  $p_a$ , and  $p_r$ ) at each generation and keeping successful changes.<sup>34</sup> Successful changes are explored using simulated annealing,<sup>35,36</sup> based on the merit of the network (see below). We use a multiplicative logarithmic cooling schedule:  $T_0/(1 + a \log(1 + i))$ , where  $i$  is the iteration number,  $T_0 = 0.1$  is the initial “temperature,” and  $a = 9.0$ .

Our optimized networks are compared with the scale-free networks and random networks of the same average degree used in previous work.<sup>7</sup> We use the linearly shifted preferential

attachment algorithm<sup>37–39</sup> to generate parametric scale-free networks—replicating the previous GNM procedure.<sup>7</sup> Erdős-Rényi random graphs<sup>40</sup> with  $\langle k \rangle = 4$  are also generated in the same manner as previous work.<sup>7</sup>

## C. Merit of health and longevity

For every iteration of our optimization algorithm, we generate a network and simulate a population of  $10^4$  individuals following Farrell *et al.*<sup>7</sup> The average lifespan ( $t_d$ ) of these individuals is measured together with health.

Aging health is measured using the frailty index (FI),<sup>10,41</sup> which is the proportion of damaged binary deficits—in our case damaged nodes. We use FI to assemble an individual QALY (quality adjusted life years) health span measure<sup>23</sup>

$$\text{QALY} = \int_0^{t_d} (1 - FI(t)) dt. \quad (4)$$

Since  $FI$  measures lack of health,  $1 - FI$  measures health. The QALY is the number of healthy years of life and is a convenient health span measure.

While assessing network complexity can be challenging,<sup>42</sup> we simply assess the network entropy of the degree correlation matrix  $P(k', k)$ ,

$$S = - \sum_{k,k'} P(k', k) \log P(k', k), \quad (5)$$

using the Shannon entropy.<sup>43</sup> Here,  $P(k', k)$  is the joint connection matrix  $J(k', k)$  of the network with a normalizing constant. While the degree distribution entropy has been used for network optimization,<sup>44</sup> previous work on the GNM emphasized the importance of nearest neighbor and degree assortativity on the health performance in the model.<sup>7</sup> We calculate the entropy on  $P(k, k')$  because it captures the degree assortativity in the network.

While entropy maximization<sup>27,28</sup> motivates our approach, for computational convenience, we impose a target entropy  $S^*$  and maximize the health performance  $H$  (which is either  $\langle t_d \rangle$  or QALY, both measured in years). Specifically, we maximize the merit,

$$M = -\lambda |S - S^*| + (1 - \lambda) \langle H \rangle, \quad (6)$$

where  $\lambda \in [0, 1]$  is a hyperparameter used for tuning entropy adherence and  $S^*$  is a target entropy that is varied across the accessible range of entropies. Our results represent the best performing  $H$  at different values of the entropy  $S^*$ ; we show results for optimizations that reach within 5% of the highest merit networks at the given entropy. We use the convex hull calculated across the top performing networks to determine the relevant optimal merit at a given entropy.

## D. Workflow summary

Our workflow is summarized in Fig. 1, which starts from the degree distribution (a), generates the joint distribution with constraints (b), generates a network (c), runs individual aging simulations using the same network (d) to obtain population health and mortality statistics, evaluates the merit (e), and explores and

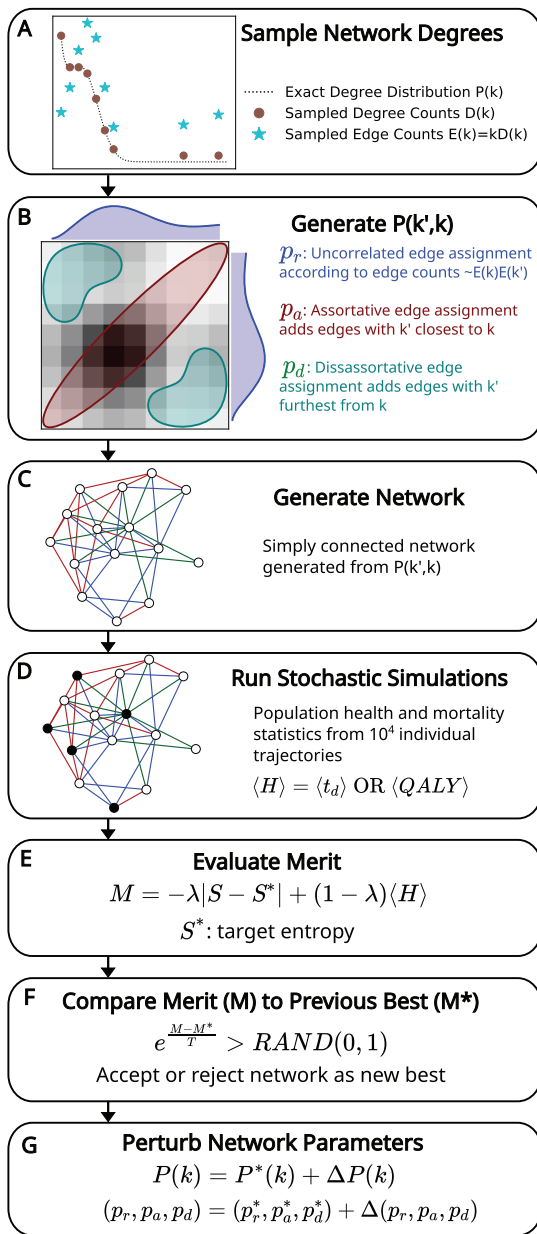


**FIG. 1.** Workflow diagram. (a) The degree distribution  $P(k)$  is sampled using the random hubs method (parametric scale-free networks instead use the preferential attachment method to generate a degree sequence based on  $\alpha$ ); (b) edges are assigned between nodes of degree  $k$  and nodes of degree  $k'$  according to the assortativity parameters  $p_a$ ,  $p_d$ , and  $p_r$ . This generates the degree correlation matrix  $P(k', k)$ ; (c) networks are generated using  $P(k', k)$  using the algorithms developed by Gjoka *et al.*;<sup>33</sup> (d) the GNM simulates the health trajectories of  $10^4$  individuals until mortality, and summary health statistics are measured; (e) merit is evaluated dependent on the entropy target  $S^*$  and the entropy weighting  $\lambda$ ; (f) the network is accepted or rejected as the new highest performing network according to simulated annealing procedures; (g) the network generation parameters are perturbed from the highest performing parameters, and the workflow is repeated with the perturbed parameters.

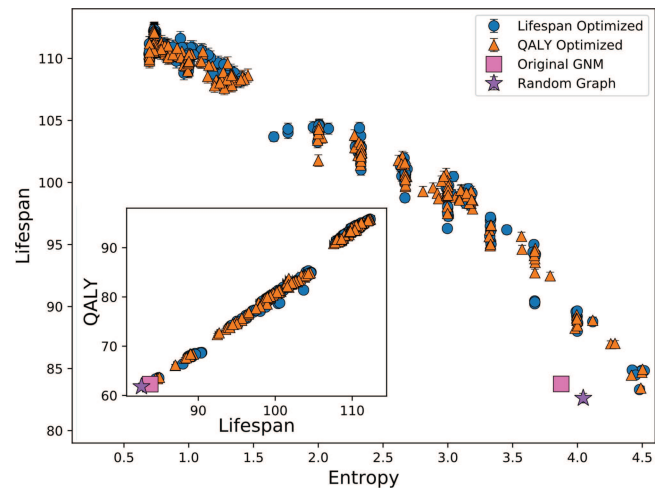


**FIG. 2.** Average lifespan for networks optimized in either lifespan ( $\langle t_d \rangle$ , blue circles) or health span (QALY, orange triangles) vs entropy  $S^*$ . Note the similar performance of the lifespan and health span optimized networks. For reference, we show a scale-free network from the GNM (pink square) and a random graph (purple star). Each point shows the endpoint of a different optimization with a network size of  $N = 1024$  nodes and an average calculated over  $10^4$  individuals for (QALY) and  $\langle t_d \rangle$ . Only networks within 5% of the best merit at a given entropy are shown. Inset: health span plotted against lifespan for the same networks.

optimizes the network parameters using simulated annealing [(f) and (g)].

### III. RESULTS

The optimized average lifespan ( $\langle t_d \rangle$ ) vs network entropy  $S^*$  is shown in Fig. 2. Networks within 5% of the maximal merit at a given  $S^*$  are shown, along with the published GNM (pink square)<sup>7</sup> and a random graph (purple star). Interestingly, the maximal average lifespan is not far above current human population averages ( $\approx 80$  yr) and is close to the maximum observed human lifespans ( $\approx 110$  yr).<sup>24</sup>

We have also shown (orange triangles) the average lifespan ( $\langle t_d \rangle$ ) of networks that were QALY optimized. They are qualitatively indistinguishable from lifespan optimized networks. While the health span is necessarily smaller than the lifespan, the inset shows that the relationship between QALY and lifespan is approximately linear for optimized networks.

Lifespan or health span optimized networks are low entropy. As indicated on the left side of Fig. 3, they are characterized by a hub and peripheral node style structure and are very disassortative. The maximum degree nodes are connected to the minimum degree nodes and there are no intermediate degree nodes.

Without any constraints, we find that the network with the best health and lifespan performance is a perfect star motif—one high-degree hub node connected to many degree 1 neighbors—with an average lifespan of 150 yr and a QALY of 120 yr (not shown). For this motif, the damage rates of peripheral nodes are only determined by the hub node—so they remain at the basal damage rate  $\Gamma_0$  until the hub node is damaged. Conversely, the hub node also remains close to its basal damage rate until a significant number of

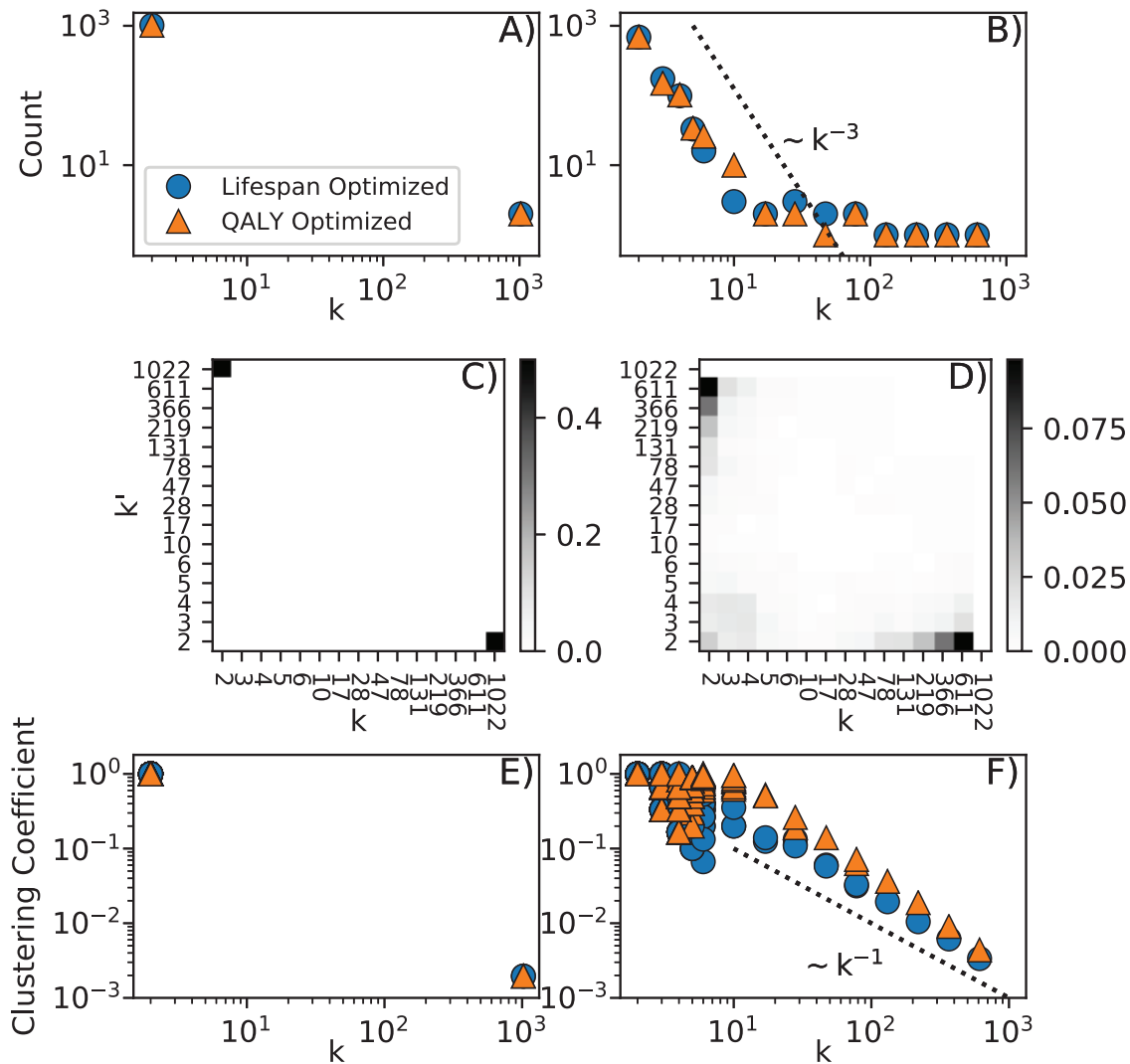


**FIG. 3.** Connectivity statistics for networks optimized at the minimum target entropy of  $S^* \approx 0.7$  [left column, panels (a), (c), and (e)] and comparable entropy to previous GNM networks  $S^* \approx 4.0$  [right side, panels (b), (d), (f)]. The top row shows the degree distributions of networks optimized for lifespan (blue circles) and QALY (orange triangles). The middle row shows the degree correlation matrices for the lifespan optimized networks. The higher entropy network maintains highly disassortative connections, but with a broader range of node degrees. Also, low-degree assortative connections begin appearing at higher entropies. The bottom row shows the local clustering coefficient  $C(k)$  for the respective networks—with the  $C(k) \sim k^{-1}$  scaling commonly observed in scale-free networks.<sup>45</sup>

peripheral nodes are damaged. Mortality occurs very soon after the hub node damages, since then the peripheral nodes rapidly damage. The average degree constraint ( $\langle k \rangle = 4$ ) prevents the optimized networks from being perfect star motifs, as does the target entropy.

At larger target entropies (and with  $\langle k \rangle = 4$ ), the hub and peripheral structure is qualitatively preserved—as can be seen in the joint degree distribution  $P(k, k')$  (Fig. 3 middle row). Strikingly, for  $S^* \gtrsim 2$ , a scale-free (power-law) degree distribution  $P(k)$  is observed at smaller  $k$ . We also find that our optimized networks have the local clustering coefficient scaling with  $k^{-1}$ , similar to real-world scale-free networks.<sup>45</sup>

Parametric scale-free networks can be efficiently generated with different degree exponents  $\alpha$  using the preferential attachment algorithm—which controls many network characteristics. As we can see with the blue circles in Fig. 4, the lifespan (and health span, not shown) are very close to the non-parametric optimization (orange triangles)—though somewhat lower. The inset shows that  $\alpha$  increases with higher network entropy. The scale-free networks also have a higher achievable maximum entropy since they are not constrained to a small number of possible degrees. Note that we have optimally rewired both the parametric and non-parametric scale-free networks with assortativity parameters ( $p_d, p_a$ , and  $p_r$ ). As

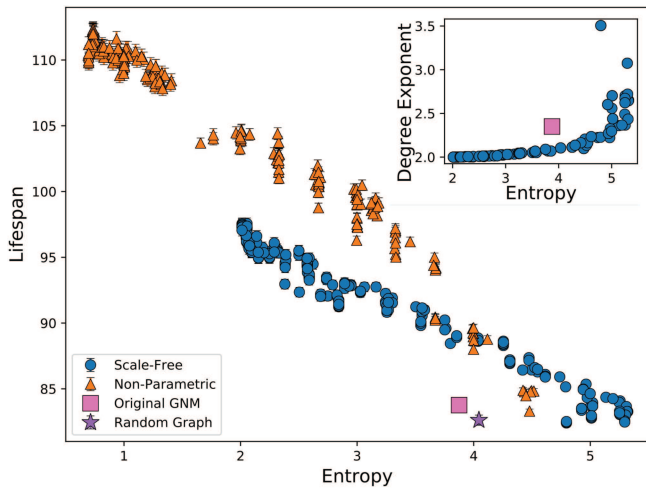


**FIG. 4.** The lifespan of networks optimized for lifespan vs target entropy  $S^*$ . The data shown are from our non-parametric optimization (orange triangles) and our tuned scale-free networks (blue circles) of size  $N = 1024$ . The non-parametric optimization reaches higher maximum lifespans and has a steeper trade-off with entropy. The scale-free networks have higher maximum entropy due to having a greater number of unique node degrees. The inset shows the parametric scale-free degree exponent  $\alpha$  along the entropy range for the same data.  $\alpha$  increases smoothly for all but the highest target entropies. For reference, we also show a scale-free network from the GNM (pink square) and a random graph (purple star).

a result of this rewiring, we find that the scale-free network originally used to model human data (pink square) falls slightly below our optimal scale-free exponent vs entropy curve.

Figure 5 shows common network metrics to assess what is changing with  $S^*$  and between parametric and non-parametric approaches. Figure 5(a) shows that there is a strong relationship between entropy and degree disassortativity. Only the non-parametric approach (triangles) can reach the lowest entropies

with maximum disassortativity—which leads to the best lifespan or health span performance. Figure 5(b) suggests that this is due to the maximum degree in the network being limited in the parametric scale-free networks (circles). Parametric scale-free networks have a similar hub and peripheral node structure as non-parametric, but since the hubs are lower degree, there are necessarily more of them. This limits disassortativity and moves further away from the ideal star motif.

Since the non-parametric optimization uses maximum degree close to  $N$  for much of the entropy range, it is helpful to look at the scaled second moment of the degree distribution to assess its top-heaviness. In Fig. 5(c), we see that the scale-free networks have smoothly decreasing second moment with entropy. However, in the non-parametric approach, there are discrete steps at lower entropies due to the transition of 2 maximum degree nodes to 1 node of maximum degree and various lower-degree hub nodes. We also find that the average clustering coefficient varies smoothly with both entropy and lifespan in these optimal networks, with the exception of some rare cases at very low entropies. We see in Fig. 5(d) that at minimum entropy, some networks flip from maximum to minimum average clustering coefficient. This is due to either the presence or absence of an edge between the maximum degree nodes, respectively.

From the network metrics, it appears that higher  $k_{max}$  leads to better lifespan and health span performance. We investigate  $k_{max}$  effects systematically by hand-building networks in the optimal lifespan hub and peripheral node structure and varying the degree of the hub nodes, while keeping  $k_{min} = 2$  and  $\langle k \rangle = 4(1 - 1/k_{max}) \simeq 4$ . Figure 6 shows how strong of an effect  $k_{max}/N$  has on both life and health span. Interestingly, health span increases more rapidly with  $k_{max}$  than lifespan. In the inset, we show that larger  $k_{max}/N$  results in delayed damage accumulation, i.e., morbidity compression.<sup>46</sup>

#### IV. DISCUSSION

Using the stochastic dynamics of the Generic Network Model (GNM) of aging and mortality, we find that the optimized network topology for maximizing either lifespan or health span is a highly

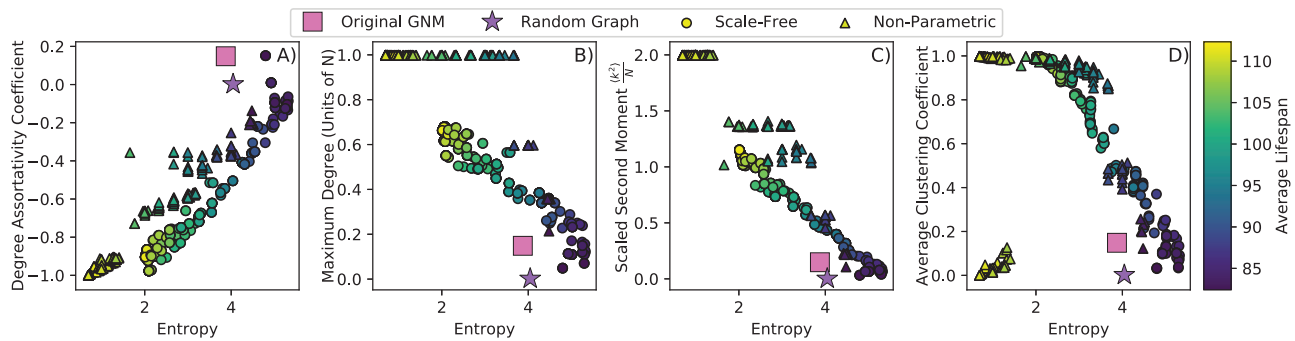


**FIG. 5.** Summary metrics for networks optimized for lifespan using our non-parametric (triangles) and scale-free (circles) methods, representing the same networks as in Fig. 4. The colors show the average lifespan of the associated network. (a) Degree assortativity vs  $S^*$ . The lowest entropy (best performing) networks are the most disassortative. (b) Maximum degree vs  $S^*$ . The maximum degree is largest at low entropies for both optimization methods but maximized over a large range of entropies in the non-parametric case. (c) The scaled second moment of degree distribution  $\langle k^2 \rangle / N$  vs  $S^*$ . The degree distributions of the networks become less top-heavy with increasing entropy, even for networks with the same maximum degree. (d) Average clustering coefficient vs  $S^*$ . The clustering coefficient generally decreases with entropy. At small entropies, some small values are observed if hub nodes are not connected directly to each other.

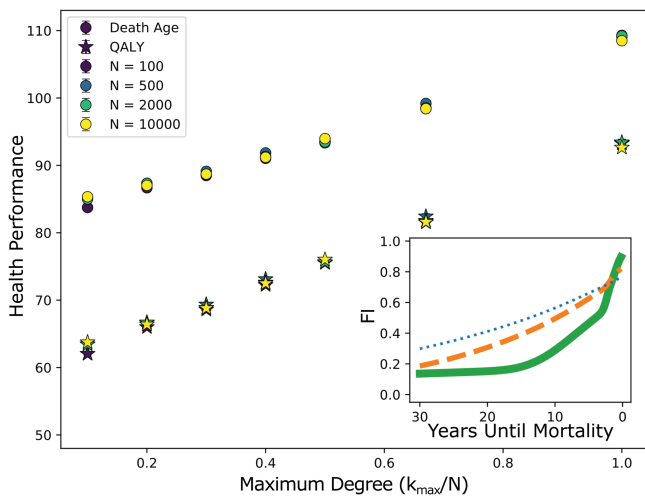


**FIG. 6.** The health performance of optimal, star motif-based networks for a range of maximum degrees  $k_{\max}/N$ . All have  $k_{\min} = 2$  and  $\langle k \rangle = 4(1 - 1/k_{\max}) \simeq 4$ . The lifespan (circles) and QALY (stars) performance of these networks increases roughly linearly for  $k_{\max}$  ranging from 10% up to 100% of the network size. The linear trend holds for the whole range of network sizes, shown by the color of the points. The inset shows the average FI (health) for the last 30 years of life for  $k_{\max}/N \approx 1$  (solid green line),  $k_{\max}/N \approx 0.5$  (dashed orange), and  $k_{\max}/N \approx 0.1$  (dotted blue). Compression of morbidity (a delayed increase of FI) is observed for larger  $k_{\max}/N$ .

disassortative and scale-free-like network. The same network optimizes both health span, as measured by the QALY, and lifespan. Without a target entropy  $S^*$  representing physiological constraints, a maximally disassortative “star” motif was optimal.

Scale-free networks with a wide range of degree assortativities are needed to model the phenomenology of human health. These networks capture a broad range of mutual-information observed between observed health attributes and mortality while simultaneously describing population health and mortality statistics.<sup>5–7</sup> As such, our optimized networks are qualitatively consistent with earlier GNM models. However, our optimization study indicates that strongly disassortative (tuned by  $p_a$  and  $p_d$ ) scale-free networks perform better than GNM networks that are generated from default preferential attachment algorithms for scale-free networks.

Since physiological constraints are represented by a generic target entropy  $S^*$  within the context of the GNM we do not test detailed theories of aging.<sup>19,20</sup> However, health span optimization is broadly consistent with life history theories that maximize reproductive success.<sup>47</sup> As such, we provide a rationale for using disassortative scale-free topologies in network models of organismal aging. It will be interesting to pursue larger-scale empirical determination of network models of aging,<sup>8</sup> since earlier analysis<sup>7</sup> was consistent with a disassortative hub-like wiring. Obtaining empirical networks at the scale required for good determination of topology may be challenging<sup>8</sup>—though finite size analysis may help.<sup>16</sup>

In contrast, cellular-scale interactome networks<sup>13,48</sup> are relatively well characterized because of the availability of high-throughput techniques. The GNM networks we have studied differ

because they represent how significant dysfunction propagates at all organismal scales, rather than representing functional interaction at cellular scales. The GNM network is static and damage propagates across it dynamically. In contrast, interactome networks change with disease or dysfunction (see, e.g., Refs. 49–51). The connection between interactome networks and the GNM dysfunction networks of this work is not yet clear.

Observational health and mortality studies of human populations implicitly include significant medical interventions. The life expectancy of people over 65 has almost doubled from 1900 to today.<sup>46</sup> We expect such medical interventions to affect the GNM dynamics (e.g., repairing damage) but not change the network topology (i.e., the interdependencies of organismal physiology). As such, our optimized network topology should still be relevant to model observed human health and mortality data.

For the underlying maximally disassortative star motif, damage typically builds up in peripheral nodes, then propagates to hub nodes, which quickly saturates the damage of peripheral nodes, which leads to mortality. Extending health span would then broadly target peripheral nodes with either budgeted repair (the “disposable soma” theory of aging<sup>19,20</sup>) or preventative health measures such as exercise<sup>52</sup> or diet.<sup>53,54</sup> Damaged hub nodes would need to be repaired rapidly before damage saturates peripheral nodes. With the network entropy constraint, the optimal network is still highly disassortative but hierarchically clustered. This scale-free behavior suggests that at all scales there will be downstream effects to consider—not just from hubs. The same lessons apply, however: broad preventative measures for peripheral nodes and rapid treatment of highly connected nodes. Wait-time effects of delayed repair would be interesting to study as part of a broader model of the effects of health interventions in the context of our optimal network structure.

The network entropy we have constrained is not the same as the thermodynamic entropy generated by organismal dysfunction during aging<sup>30</sup> or the genomic entropy accumulated during aging.<sup>29</sup> However, the network determines how dysfunction propagates—and so determines where thermodynamic entropy is generated and where the effects of genomic damage and dysregulation are observed.

For our GNM, simplifying assumptions are that the dynamical rate constants ( $\gamma^+$ ,  $\Gamma_0$ ) do not vary among nodes and that edges between nodes are unweighted and undirected—i.e., that the dynamical parameters are homogeneous. In real systems, we would expect rate constants to vary between nodes and interaction strengths to vary between edges—i.e., to have heterogeneous weights. Heterogeneous weights could be reconstructed with sufficient observational data,<sup>8</sup> and nodes could then be identified with specific physiological features. We further note that the health attributes in the GNM are binary, which is common practice in healthcare. Some progress has been made in reconstructing heterogeneous interaction networks of continuous aging variables using deep-learning techniques.<sup>2</sup> Optimizing heterogeneous networks—with either binary or continuous variables—would be a daunting prospect because the heterogeneity leads to a huge parameter space and a consequent curse of dimensionality. More practically, sufficiently large reconstructed heterogeneous networks should allow us to examine whether the network structures we recover here are observed in practice.

One important result is that health span and lifespan optimization are equivalent. Accordingly, health span (the compression of morbidity) is how lifespan is maximized. This is largely determined by high disassortativity—a specialized hub-like network structure where hubs are more strongly connected to peripheral nodes than each other. Qualitatively this looks much like the organismal structure we observe. Because our approach is generic, we would obtain the same results for other organisms or sub-system that maximizes its health span. Accordingly, we expect that many biological organisms and their constituent subsystems to exhibit disassortative star-like or scale-free structures at every scale—subject to any detailed physiological constraints.

## ACKNOWLEDGMENTS

We thank ACENET and the Digital Research Alliance of Canada for computational support and resources, and Spencer Farrell for helpful discussions. A.R. acknowledges the Natural Sciences and Engineering Research Council (NSERC) for operating Grant No. RGPIN-2019-05888.

## AUTHOR DECLARATIONS

### Conflict of Interest

The authors have no conflicts to disclose.

## Author Contributions

**Garrett Stubbings:** Conceptualization (equal); Investigation (lead); Methodology (equal); Writing – original draft (lead); Writing – review & editing (equal). **Andrew Rutenberg:** Conceptualization (equal); Funding acquisition (lead); Methodology (equal); Supervision (lead); Writing – original draft (supporting); Writing – review & editing (equal).

## REFERENCES

- <sup>1</sup>X. Li, A. Ploner, Y. Wang, P. K. Magnusson, C. Reynolds, D. Finkel, N. L. Pedersen, J. Jylhävä, and S. Hägg, “Longitudinal trajectories, correlations and mortality associations of nine biological ages across 20-years follow-up,” *eLife* **9**, 132 (2020).
- <sup>2</sup>S. Farrell, A. Mitnitski, K. Rockwood, and A. Rutenberg, “Interpretable machine learning for high-dimensional trajectories of aging health,” *PLoS Comput. Biol.* **18**, e1009746 (2022).
- <sup>3</sup>L. A. Gavrilov and N. S. Gavrilova, “The reliability theory of aging and longevity,” *J. Theor. Biol.* **213**, 527 (2001).
- <sup>4</sup>D. C. Vural, S. Morrison, and L. Mahadevan, “Aging in complex interdependency networks,” *Phys. Rev. E* **89**, 022811 (2014).
- <sup>5</sup>S. Taneja, A. B. Mitnitski, K. Rockwood, and A. D. Rutenberg, “Dynamical network model for age-related health deficits and mortality,” *Phys. Rev. E* **93**, 022309 (2016).
- <sup>6</sup>S. G. Farrell, A. B. Mitnitski, K. Rockwood, and A. D. Rutenberg, “Network model of human aging: Frailty limits and information measures,” *Phys. Rev. E* **94**, 052409 (2016).
- <sup>7</sup>S. G. Farrell, A. B. Mitnitski, O. Theou, K. Rockwood, and A. D. Rutenberg, “Probing the network structure of health deficits in human aging,” *Phys. Rev. E* **98**, 032302 (2018).
- <sup>8</sup>S. Farrell, A. Mitnitski, K. Rockwood, and A. Rutenberg, “Generating synthetic aging trajectories with a weighted network model using cross-sectional data,” *Sci. Rep.* **10**, 19833 (2020).
- <sup>9</sup>T. B. L. Kirkwood, “Deciphering death: A commentary on Gompertz (1825) ‘On the nature of the function expressive of the law of human mortality, and on a new

mode of determining the value of life contingencies,” *Philos. Trans. R. Soc. B* **370**, 20140379 (2015).

- <sup>10</sup>A. B. Mitnitski, A. J. Mogilner, and K. Rockwood, “Accumulation of deficits as a proxy measure of aging,” *Sci. World J.* **1**, 323 (2001).
- <sup>11</sup>A. Mitnitski and K. Rockwood, “Aging as a process of deficit accumulation: Its utility and origin,” *Interdiscip. Top. Gerontol.* **40**, 85–98 (2015).
- <sup>12</sup>Y. I. Wolf, G. Karev, and E. V. Koonin, “Scale-free networks in biology: New insights into the fundamentals of evolution?,” *BioEssays* **24**, 105 (2002).
- <sup>13</sup>A.-L. Barabási and Z. N. Oltvai, “Network biology: Understanding the cell’s functional organization,” *Nat. Rev. Genet.* **5**, 101–113 (2004).
- <sup>14</sup>A.-L. Barabási, “Scale-free networks: A decade and beyond,” *Science* **325**, 412–413 (2009).
- <sup>15</sup>A. D. Broido and A. Clauset, “Scale-free networks are rare,” *Nat. Commun.* **10**, 1017 (2019).
- <sup>16</sup>M. Serafino, G. Cimini, A. Maritan, A. Rinaldo, S. Suweis, J. R. Banavar, and G. Caldarelli, “True scale-free networks hidden by finite size effects,” *Proc. Natl. Acad. Sci. U.S.A.* **118**, e2013825118 (2021).
- <sup>17</sup>A.-L. Barabási and E. Bonabeau, “Scale-free networks,” *Sci. Am.* **288**, 60 (2003).
- <sup>18</sup>M. P. H. Stumpf and M. A. Porter, “Critical truths about power laws,” *Science* **335**, 665–666 (2012).
- <sup>19</sup>L. A. Gavrilov and N. S. Gavrilova, “Evolutionary theories of aging and longevity,” *Sci. World J.* **2**, 339–356 (2002).
- <sup>20</sup>T. B. Kirkwood, “Understanding the odd science of aging,” *Cell* **120**, 437–447 (2005).
- <sup>21</sup>L. Demetrius, S. Legendre, and P. Harremöes, “Evolutionary entropy: A predictor of body size, metabolic rate and maximal life span,” *Bull. Math. Biol.* **71**, 800 (2009).
- <sup>22</sup>E. M. Crimmins, “Lifespan and healthspan: Past, present, and promise,” *Gerontologist* **55**, 901 (2015).
- <sup>23</sup>M. R. Gold, D. Stevenson, and D. G. Fryback, “HALYS and QALYS and DALYS, oh my: Similarities and differences in summary measures of population health,” *Annu. Rev. Public Health* **23**, 115–134 (2002).
- <sup>24</sup>X. Dong, B. Milholland, and J. Vijg, “Evidence for a limit to human lifespan,” *Nature* **538**, 257–259 (2016).
- <sup>25</sup>A. Lenart and J. W. Vaupel, “Questionable evidence for a limit to human lifespan,” *Nature* **546**, E13–E14 (2017).
- <sup>26</sup>L. A. Gavrilov and N. S. Gavrilova, “Late-life mortality is underestimated because of data errors,” *PLoS Biol.* **17**, e3000148 (2019).
- <sup>27</sup>S. Pressé, K. Ghosh, J. Lee, and K. A. Dill, “Principles of maximum entropy and maximum caliber in statistical physics,” *Rev. Mod. Phys.* **85**, 1115–1141 (2013).
- <sup>28</sup>A. Lesne, “Shannon entropy: A rigorous notion at the crossroads between probability, information theory, dynamical systems and statistical physics,” *Math. Struct. Comput. Sci.* **24**, e240311 (2014).
- <sup>29</sup>J. E. Riggs, “Aging, increasing genomic entropy, and neurodegenerative disease,” *Neurol. Clinics* **16**, 757–770 (1998).
- <sup>30</sup>Z. Wang, “The entropy perspective on human illness and aging,” *Engineering* **9**, 22–26 (2022).
- <sup>31</sup>D. R. Cox, “Regression models and life-tables,” *J. R. Stat. Soc., Ser. B* **34**, 187 (1972).
- <sup>32</sup>M. L. Bertotti and G. Modanese, “The configuration model for Barabasi-Albert networks,” *Appl. Network Sci.* **4**, 1 (2019).
- <sup>33</sup>M. Gjoka, B. Tillman, and A. Markopoulou, “Construction of simple graphs with a target joint degree matrix and beyond,” in *2015 IEEE Conference on Computer Communications (INFOCOM) (IEEE, 2015)*, pp. 1553–1561.
- <sup>34</sup>T. Bäck and H.-P. Schwefel, “An overview of evolutionary algorithms for parameter optimization,” *Evol. Comput.* **1**, 1 (1993).
- <sup>35</sup>P. J. Van Laarhoven and E. H. Aarts, “Simulated annealing,” in *Simulated Annealing: Theory and Applications* (Springer, 1987), pp. 7–15.
- <sup>36</sup>E. Aarts and J. Korst, *Simulated Annealing and Boltzmann Machines: A Stochastic Approach to Combinatorial Optimization and Neural Computing* (John Wiley & Sons, Inc., 1989).
- <sup>37</sup>A.-L. Barabási and R. Albert, “Emergence of scaling in random networks,” *Science* **286**, 509 (1999).

- <sup>38</sup>P. L. Krapivsky and S. Redner, "Organization of growing random networks," *Phys. Rev. E* **63**, 066123 (2001).
- <sup>39</sup>B. Fotouhi and M. G. Rabbat, "Degree correlation in scale-free graphs," *Eur. Phys. J. B* **86**, 510 (2013).
- <sup>40</sup>A.-L. Barabási and M. Pósfai, *Network Science* (Cambridge University Press, 2016).
- <sup>41</sup>S. D. Searle, A. Mitnitski, E. A. Gahbauer, T. M. Gill, and K. Rockwood, "A standard procedure for creating a frailty index," *BMC Geriatr.* **8**, 24 (2008).
- <sup>42</sup>M. Morzy, T. Kajdanowicz, and P. Kaziemko, "On measuring the complexity of networks: Kolmogorov complexity versus entropy," *Complexity* **2017**, 1 (2017).
- <sup>43</sup>C. E. Shannon, "A mathematical theory of communication," *The Bell Syst. Tech. J.* **27**, 379 (1948).
- <sup>44</sup>R. F. I. Cancho and R. V. Solé, "Optimization in complex networks," in *Statistical Mechanics of Complex Networks* (Springer, Berlin, 2003), pp. 114–126.
- <sup>45</sup>E. Ravasz and A.-L. Barabási, "Hierarchical organization in complex networks," *Phys. Rev. E* **67**, 026112 (2003).
- <sup>46</sup>J. F. Fries, B. Bruce, and E. Chakravarty, "Compression of morbidity 1980–2011: A focused review of paradigms and progress," *J. Aging Res.* **2011**, 261702 (2011).
- <sup>47</sup>S. C. Stearns, "Life history evolution: Successes, limitations, and prospects," *Naturwissenschaften* **87**, 476–486 (2000).
- <sup>48</sup>A.-L. Barabási, N. Gulbahce, and J. Loscalzo, "Network medicine: A network-based approach to human disease," *Nat. Rev. Genet.* **12**, 56–68 (2011).
- <sup>49</sup>A. Rai, P. Shinde, and S. Jalan, "Network spectra for drug-target identification in complex diseases: New guns against old foes," *Appl. Network Sci.* **3**, 51 (2018).
- <sup>50</sup>A. Rai, P. Pradhan, J. Nagraj, K. Lohitesh, R. Chowdhury, and S. Jalan, "Understanding cancer complexome using networks, spectral graph theory and multilayer framework," *Sci. Rep.* **7**, 41676 (2017).
- <sup>51</sup>P. Shinde, A. Yadav, A. Rai, and S. Jalan, "Dissortativity and duplications in oral cancer," *Eur. Phys. J. B* **88**, 197 (2015).
- <sup>52</sup>D. Lee, R. R. Pate, C. J. Lavie, X. Sui, T. S. Church, and S. N. Blair, "Leisure-time running reduces all-cause and cardiovascular mortality risk," *J. Am. Coll. Cardiol.* **64**, 472 (2014).
- <sup>53</sup>M. R. Entwistle, D. Schweizer, and R. Cisneros, "Dietary patterns related to total mortality and cancer mortality in the united states," *Cancer Causes Control* **32**, 1279–1288 (2021).
- <sup>54</sup>M. J. Claesson, I. B. Jeffery, S. Conde, S. E. Power, E. M. O'Connor, S. Cusack, H. M. B. Harris, M. Coakley, B. Lakshminarayanan, O. O'Sullivan *et al.*, "Gut microbiota composition correlates with diet and health in the elderly," *Nature* **488**, 178–184 (2012).